

Direct Observation of Superheating and Supercooling of Vortex Matter using Neutron Diffraction

X. S. Ling,¹ S. R. Park,¹ B. A. McClain,¹ S. M. Choi,^{2,3} D. C. Dender,^{2,3} and J. W. Lynn²

¹*Department of Physics, Brown University, Providence, Rhode Island 02912*

²*NIST Center for Neutron Research, Gaithersburg, Maryland 20899*

³*University of Maryland, College Park, Maryland 20742*

Abstract

We report the first observation of a striking history dependence of the structure function of the vortex matter in the peak effect regime in a Nb single crystal by using small angle neutron scattering combined with *in situ* magnetic susceptibility measurements. Metastable phases of vortex matter, supercooled vortex liquid and superheated vortex solid, have been identified. We interpret our results as direct structural evidence for a first-order solid-liquid transition at the peak effect.

PACS numbers: 74.60.Ge, 61.12.Ex

A current subject of wide interest concerns the existence of a vortex solid-liquid transition in type-II superconductors [1]. In addition to providing a model system for the study of melting and freezing, the vortex matter system offers unprecedented opportunities in studying the effects of quenched disorder on phase transitions. Recently, the magnetization jump in high- T_c superconductors $\text{YBa}_2\text{Cu}_3\text{O}_{7-\delta}$ (YBCO), a widely accepted thermodynamic signature of a vortex solid-liquid transition [2], and the peak effect, a well-known vortex-lattice softening anomaly in many low- T_c [3,4] and high- T_c [5–8] superconductors in which the critical current exhibits a peak rather than decreasing monotonically with increasing temperature, are found to occur at the same temperature [7,8]. However, there is no direct structural evidence indicating whether the underlying phase transition is solid-to-solid, solid-to-liquid, or even liquid-to-liquid in origin. Since quenched disorder is known to have important consequences for phase transitions [9,10], whether a solid-liquid transition can occur when random pinning is effective has broad implications in condensed matter physics.

Small angle neutron scattering (SANS) [11–15] is presently the most powerful technique for probing the vortex structure in bulk superconductors. For high- T_c superconductors, the magnetic penetration depth is typically quite long, yielding a very weak vortex signal in SANS experiments, which has so far prevented a direct structural study of the peak effect in high- T_c systems. Recent effort has therefore focused on low- T_c systems where one can detect the peak effect and measure the vortex structure using SANS in the same temperature and field regime [14,15], and for these purposes Nb is experimentally the most favorable system because of the short penetration depth and the availability of large, ultrahigh quality single crystals. However, it has been controversial as to whether there is a vortex solid-liquid transition in Nb and the two previous SANS studies of this issue were not conclusive

[14,15]. In the first study [14], a characteristic temperature at which the azimuthal width of the Bragg peaks starts to increase was interpreted as the vortex-lattice melting transition. In the second study [15], a nearly isotropic ring of scattering was observed in the peak-effect regime, but was interpreted as a disordered solid rather than a liquid. In both studies, only field-cooled vortex states were measured. We report here striking hysteresis in neutron diffraction patterns of the vortex state in the peak-effect regime of Nb. The metastability of supercooled and superheated vortex states is directly demonstrated by applying a weak perturbation and observing the evolution of the SANS patterns. These data provide direct evidence for a first-order vortex solid-liquid transition.

Our experiments were performed using the 30-m SANS instrument NG-7 at the NIST Center for Neutron Research. The increased flux on the SANS instrument due to a new liquid-hydrogen cold source turns out to be important, but the key improvement provided by the present experiment is that the SANS and the ac magnetic response of the vortex array are measured simultaneously *in situ*. Thus one can correlate the ordering in the vortex state directly with the macroscopic vortex dynamics. The coil for the magnetic ac susceptibility measurements can also be used to apply a small ac field to dynamically perturb the vortex system, allowing an *in situ* determination of the metastability of the vortex states.

The sample is a Nb single crystal of 99.998% purity, a cylinder with a slightly uneven diameter from 1.316 cm at one end to 1.169 cm at the other, and 2.48 cm in length. The incident neutron beam has a mean wavelength $\lambda=6.0$ Å and a bandwidth $\Delta\lambda/\lambda=0.11$. The neutron beam traverses through the central region of the sample, defined by a cadmium mask (0.7 cm in diameter), along the cylindrical axis which coincides with the three-fold symmetric $\langle 111 \rangle$ crystallographic direction. The dc magnetic field is applied by

a horizontal superconducting magnet along the same direction. The absolute accuracy of the measured sample temperature is ± 0.20 K with a temperature stability better than ± 0.025 K.

The peak-effect regime of the Nb sample is determined *in situ* by measuring the characteristic dip in the temperature dependence of the real-part of the ac magnetic susceptibility $\chi'(T)$, as shown in Fig.1(a) for $H=3.75$ kOe. The pronounced diamagnetic dip in $\chi'(T)$ of the ac susceptibility corresponds to a strong peak effect in the critical current (or nonlinear conductance) in the sample [5,8]. The onset, the peak, and the end of the peak effect are denoted by $T_o(H)$, $T_p(H)$, and $T_{c2}(H)$, respectively. (In YBCO, the end of the peak effect is still far below $T_{c2}(H)$ [5–8].) Fig.1(b) shows the window of our experiment. The upper critical field $H_{c2}(4.20\text{K}) = 4.23$ kOe of this sample is higher than that of Ref. [15] but similar to that of Ref. [14]. The lower critical field line, separating the Abrikosov and Meissner phases, is estimated from the first appearance of vortex scattering in the SANS.

For each (T, H) , we measure the vortex SANS patterns for different thermal paths. For low temperatures the vortex SANS images show sharp Bragg peaks with sixfold symmetry in agreement with previous studies [11,14,15], independent of the thermal history. An example is shown in the inset of Fig.1(b) for $H=3.75$ kOe and $T=3.50$ K. However, the vortex SANS pattern starts to show striking history dependence as the peak-effect regime is approached. For clarity, we define the field-cooled (FC) state as when the sample is cooled to the target temperature in a magnetic field, while the zero-field-cooled (ZFC) state is reached by cooling the sample in zero field to the target temperature and then increasing the magnetic field to the desired value. A field-cooled-warming (FC-W) state is when the system is cooled in field to a much lower temperature (~ 2 K) then warmed back to the final temperature.

For the FC path, the vortex SANS patterns show nearly isotropic rings for

$T_p < T < T_{c2}$ and broad Bragg spots for $T < T_p$. There is no clear sharpening in the Bragg peaks when T_o is crossed. Only at a lower $T < T_p$ do the Bragg peaks become sharp. In contrast, for the ZFC and the FC-W paths, the sharp Bragg spots are observed for all temperatures up to T_{c2} . Shown in the top panel of Fig.2 are the ZFC and FC images at $H=3.75$ kOe and $T=4.40$ K, which is just below $T_o(3.75\text{kOe})=4.50$ K. The images in the mid panel are for $H=4.00$ kOe and $T=4.40$ K, which is 0.10 K above $T_p(4.0\text{kOe})=4.30$ K. The intensities at the radial maximum for the mid panel SANS data are plotted in the lower panel. The sharp Bragg spots for the ZFC state indicate a vortex lattice with long-range-order (LRO) [16], while the broad spots for the FC state suggest a disordered phase with short-range-order.

The orientational order of the vortex assembly can be quantified by the azimuthal widths of the Bragg peaks at the radial position of the intensity maximum. The azimuthal widths $\Delta\theta$ of the Bragg peaks can be obtained by fitting six Gaussian peaks to the data, for each (T, H) and path. Likewise, the translational order of the vortex assembly can be quantified by the radial widths ΔQ of the Bragg peaks. The Gaussian widths are plotted in Fig.3. Clearly, the ZFC states are more ordered than the FC states, translationally and orientationally, across the peak-effect regime. To determine the positional correlation of the vortex lines along the field direction, the rocking curves (Bragg peak intensity vs. the relative angle between the neutron beam and the applied magnetic field) of the ZFC and FC states at $H=3.75$ kOe and $T=4.40$ K are also measured. The rocking-curve width for the FC state is 30% larger than that of the ZFC state, suggesting that the vortex lines are entangled [17] in the FC states, but nearly straight in the ZFC (and FC-W) states.

Since a simultaneous broadening in radial and azimuthal widths is characteristic of a liquid (or glass) [18], the hysteresis in both $\Delta\theta$ and ΔQ suggests

a first-order vortex solid-liquid (or glass) transition. A controversial issue is the location of the underlying equilibrium phase transition in the vortex matter relative to the position of the peak effect [4,19–21]. One interpretation [4,19,20] places the conjectured vortex solid-liquid transition T_m at T_p , consistent with the recent experiments [7,8] in YBCO where the magnetization jump was found to coincide with the peak effect (the two are also related in other high- T_c systems [22]). Another widely held view, is based on the classical Lindemann criterion which would place T_m at $T_{c2}(H)$ for Nb, provided the vortex-lattice elastic moduli are well-behaved [23]. In this scenario, the FC disordered phase seen here (as well as in [14,15]) is a supercooled liquid and the thermodynamic ground state is an ordered solid across the entire peak-effect regime. The third scenario places T_m at or below the onset of the peak effect [21].

We find that it is possible to experimentally determine the ground state, and consequently the approximate position of T_m , of the vortex system. For this purpose, we use the ac susceptibility coil to apply a small ac magnetic field to shake the vortex assembly and use the SANS to observe how the structure of the system evolves. Even though the true ground state of the vortex system may not have been reached in the time scale of the shaking experiment due to random pinning, the evolution of the diffraction patterns leaves little doubt regarding the nature of the ground state.

As shown in Fig.4(a), after applying an ac field of 3.3 Oe at 100 Hz (1 kHz gives similar results) for 10^3 sec, the ordered ZFC vortex lattice becomes completely disordered. Preliminary time-dependent data show that the Bragg peaks start to disappear within the first 10^2 sec of the shaking experiment. In contrast, no measurable difference can be found for the disordered FC vortex states before and after the ac field is applied (for up to 10^4 sec). By using the same approach, we find that the FC disordered states for $T < T_p$ are

metastable and the ordered ZFC state is the ground state, opposite to that for $T > T_p$. In the $T < T_p$ regime, the metastability is obviously stronger since a much larger ac field is needed to change the metastable state. We find that an ac field of 50 Oe (at ≈ 0.1 Hz, using the superconducting magnet at non-persistent mode) can crystallize the disordered FC states at $T < T_p$. The shaking effects of an ac magnetic field were also observed in transport [24] and ac magnetization [25] in the peak-effect region in 2H-NbSe₂, and were interpreted as a structural re-organization in the vortex matter, consistent with our direct SANS observations here.

The metastable nature of the ZFC ordered state for $T > T_p$ can also be observed in a field ramping experiment. For example, at a field ramp (increase) rate of less than 5 Oe/sec, the final vortex state (at $T > T_p$) is always ordered. In contrast, a ramp rate larger than 40 Oe/sec always results in a disordered state. However, the field ramping experiment alone cannot rule out a trivial possibility that the sample was heated to above $T_{c2}(H)$ during the field ramping by the induced screening current. If this happens, after the field ramping stops, the sample cools back to the set temperature *in field* and the final state is actually a FC state. In the shaking experiment, the ac susceptibility of the sample is monitored and serves as an *in situ* thermometer to ensure that the sample temperature never fluctuates to above $T_{c2}(H)$ during the entire SANS run (1 hour).

Thus we conclude that, for $T > T_p$, the ordered ZFC vortex lattice is a superheated state and the ground state of the vortex system is a disordered vortex liquid, while for $T < T_p$, the ground state is a vortex crystal (or Bragg glass [16]), and the disordered FC state is a supercooled vortex liquid. A thermodynamic phase transition must have taken place in the region of the peak effect, $T_m \approx T_p$. This is consistent with the observations in YBCO where the magnetization jump was found to coincide with the peak

effect [7,8]. In principle, one should also observe a discontinuous change of Q_o when the vortex solid melts. Unfortunately, the expected shift in Q_o due to the density change at the vortex solid-liquid transition is below our resolution limit, as we estimate here. From thermodynamic considerations [2], using the Clausius-Clapeyron relations, the vortex density change at T_m is of the order $\Delta B = -\frac{4\pi c_L^2 C_{66}}{T_m dH_m/dT}$ where c_L is the Lindemann number and $C_{66} \approx \frac{B_{c2}^2}{4\pi} \frac{b(1-b)^2}{8\kappa^2}$ is the vortex-lattice shear modulus, $b = B/B_{c2}$. For Nb at $H=4.00$ kOe, $T_m \approx T_p=4.30$ K ($T_{c2}=4.50$ K), $dH_m/dT = -0.846$ kOe/K, and $C_{66} \approx 0.6 \times 10^4$ erg/cm³ assuming a reasonable $\kappa \approx 1$ and Lindemann number $c_L=0.1$, the upper bound for the jump ΔB at melting is about 0.2 G. For a triangular lattice before melting $Q_o(B = H) = 2\pi \sqrt{\frac{2}{\sqrt{3}}} \sqrt{\frac{H}{\phi_o}}$, the expected $\Delta Q_o \approx 3 \times 10^{-5} Q_o$ which is far too small to be resolved by the present SANS instruments. In Fig.4(b), the radial peak position Q_o remains unchanged after shaking-induced melting, consistent with the above estimate.

Another interesting feature in Fig.3 is that there appears to be a characteristic temperature below which the vortex state is insensitive to its thermal history. For example, at $H=3.75$ kOe, the FC, ZFC, and FC-W states at 3.50 K are all ordered. The crossover temperature, $t \approx 0.85$ in Fig.3, is in fact very close to the melting line identified previously [14] (which was based on the measurements of the FC states). We interpret this temperature as the lower limit for supercooling.

A closer examination of the diffuse scattering rings in Figs.1&2 suggests that they are not completely isotropic, indicating some short-range correlations. We attribute this short-range order to the coupling of the vortex liquid to the atomic crystal lattice, since experimentally one finds that in the Bragg solid phase, the specific orientation of the vortex lattice is always fixed to a certain crystallographic orientation of the sample. (This is the case for all low- T_c and high- T_c systems [13].) In the supercooled state (top-right in Fig.

2), the highly correlated vortex liquid [14], reminiscent of the hexatic liquid phase in 2D melting [26], is also likely related to this coupling.

We point out that our results imply the absence of superheating in conventional transport experiments with a large drive current. This solves a well-known puzzle [27,28] in which the history dependence of the nonlinear resistance always vanishes at $T_p(H)$. Only with extremely low drive currents may one observe the subtle effects of superheating in transport [29]. The superheating of vortex solid contrasts sharply with that in regular bulk solids where surface melting prevents superheating [30]. Surface melting of vortex solid is likely suppressed by the surface barrier [29] in type-II superconductors.

In summary, we have observed a striking hysteresis in the SANS patterns of the vortex matter in the peak effect regime of a high quality Nb single crystal. The FC vortex states are disordered across the entire peak effect region and can be supercooled to below the onset of the peak effect. In contrast, the ZFC or the FC-W vortex states are ordered up to $H_{c2}(T)$. The ordered ZFC/FC-W vortex lattices near $H_{c2}(T)$ are identified as superheated solids which can be melted (disordered) by applying a small ac magnetic field. We interpret our SANS hysteresis data as direct evidence for a first-order vortex solid-liquid (glass) transition.

We thank C.J. Glinka for assistance and J.J. Rush for providing the Nb crystal; C. Elbaum, A. Houghton, J.M. Kosterlitz, H.J. Maris, and S.C. Ying for discussions. This work was supported in part by NSF through Grant No. DMR-0075838, the A.P. Sloan Foundation (XSL), and the Brown Salomon Award program.

REFERENCES

- [1] For a review, see G. Blatter *et al.*, *Rev. Mod. Phys.* **66**, 1125 (1994).
- [2] E. Zeldov *et al.*, *Nature* **375**, 373 (1995); R. Liang, D.A. Bonn, W.N. Hardy, *Phys. Rev. Lett.* **76**, 835 (1996); U. Welp *et al.*, *ibid.*, p.4809.
- [3] S.H. Autler, E.S. Rosenblum, K. Gooen, *Phys. Rev. Lett.* **9**, 489 (1962); A.B. Pippard, *Phil. Mag.* **19**, 217 (1969); A.I. Larkin and Yu.N. Ovchinnikov, *J. Low Temp. Phys.* **34**, 409 (1979); R. Wördenweber, P.H. Kes, C.C. Tsuei, *Phys. Rev. B* **33**, 3172 (1986).
- [4] S. Bhattacharya and M.J. Higgins, *Phys. Rev. Lett.* **70**, 2617 (1993).
- [5] X.S. Ling and J.I. Budnick, in *Magnetic Susceptibility of Superconductors and Other Spin Systems*, R.A. Hein *et al.*, Eds. (Plenum Press, 1991), p.377.
- [6] W.K. Kwok *et al.*, *Phys. Rev. Lett.* **73**, 2614 (1994).
- [7] T. Ishida, K. Okuda, H. Asaoka, *Phys. Rev. B* **56**, 5128 (1997).
- [8] J. Shi *et al.*, *Phys. Rev. B* **60**, R12593 (1999).
- [9] A.I. Larkin, *Sov. Phys. JETP* **31**, 784 (1970); Y. Imry and S.-k. Ma, *Phys. Rev. Lett.* **39**, 1399 (1975)
- [10] D.S. Fisher, M.P.A. Fisher, and D.A. Huse, *Phys. Rev. B* **43**, 130 (1991).
- [11] D. Cribier, Y. Simon, P. Thorel, *Phys. Rev. Lett.* **28**, 1370 (1972); D.K. Christen *et al.*, *Phys. Rev. B* **15**, 4506 (1977).
- [12] R. Cubitt *et al.*, *Nature* **365**, 407 (1993).
- [13] B. Keimer *et al.*, *Phys. Rev. Lett.* **73**, 3459 (1994).
- [14] J.W. Lynn *et al.*, *Phys. Rev. Lett.* **72**, 3413 (1994).
- [15] P.L. Gammel *et al.*, *Phys. Rev. Lett.* **80**, 833 (1998).

- [16] Strictly speaking, the ordered vortex lattice should be a Bragg glass with quasi-LRO in translation but true LRO in orientation due to the weak random pinning centers, see T. Giamarchi and P. Le Doussal, *Phys. Rev.* **B 52**, 1242 (1995). However the present experimental resolution cannot distinguish these subtleties.
- [17] D.R. Nelson, *Phys. Rev. Lett.* **60**, 1973 (1988); M.C. Marchetti and D.R. Nelson, *Phys. Rev.* **B 41**, 1910 (1990).
- [18] Here we use the classical structural definitions of liquids and glasses (supercooled liquids), see P.M. Chaikin and T.C. Lubensky, *Principles of Condensed Matter Physics*, (Cambridge University Press, 1995). We do not rule out the possibility that the structurally disordered vortex phases are a vortex glass [10] with zero ohmic resistance.
- [19] T. Ala-Nissila, E. Granato, S.C. Ying, *J. Phys.: Cond. Matt.* **2**, 8537 (1990).
- [20] A.I. Larkin, M.C. Marchetti, V.M. Vinokur, *Phys. Rev. Lett.* **75**, 2992 (1995).
- [21] C. Tang *et al.*, *Europhys. Lett.* **35**, 597 (1996).
- [22] B. Khaykovich *et al.*, *Phys. Rev. Lett.* **76**, 2555 (1996).
- [23] A. Houghton, R.A. Pelcovits, A. Sudbø, *Phys. Rev.* **B 40**, 6763 (1989).
- [24] M.W. Rabin *et al.*, *Phys. Rev.* **B 57**, R720 (1998).
- [25] S.S. Banerjee *et al.*, *App. Phys. Lett.*, **74**, 126 (1999).
- [26] B.I. Halperin and D.R. Nelson, *Phys. Rev. Lett.* **41**, 121 (1978).
- [27] W. Henderson *et al.*, *Phys. Rev. Lett.* **77**, 2077 (1996).
- [28] X.S. Ling, J.E. Berger, D.E. Prober, *Phys. Rev.* **B 57**, R3249 (1998).
- [29] M. Charalambous *et al.*, *Phys. Rev. Lett.* **71**, 436 (1993).
- [30] F. Lund, *Phys. Rev. Lett.* **69**, 3084 (1992).

Figure Captions:

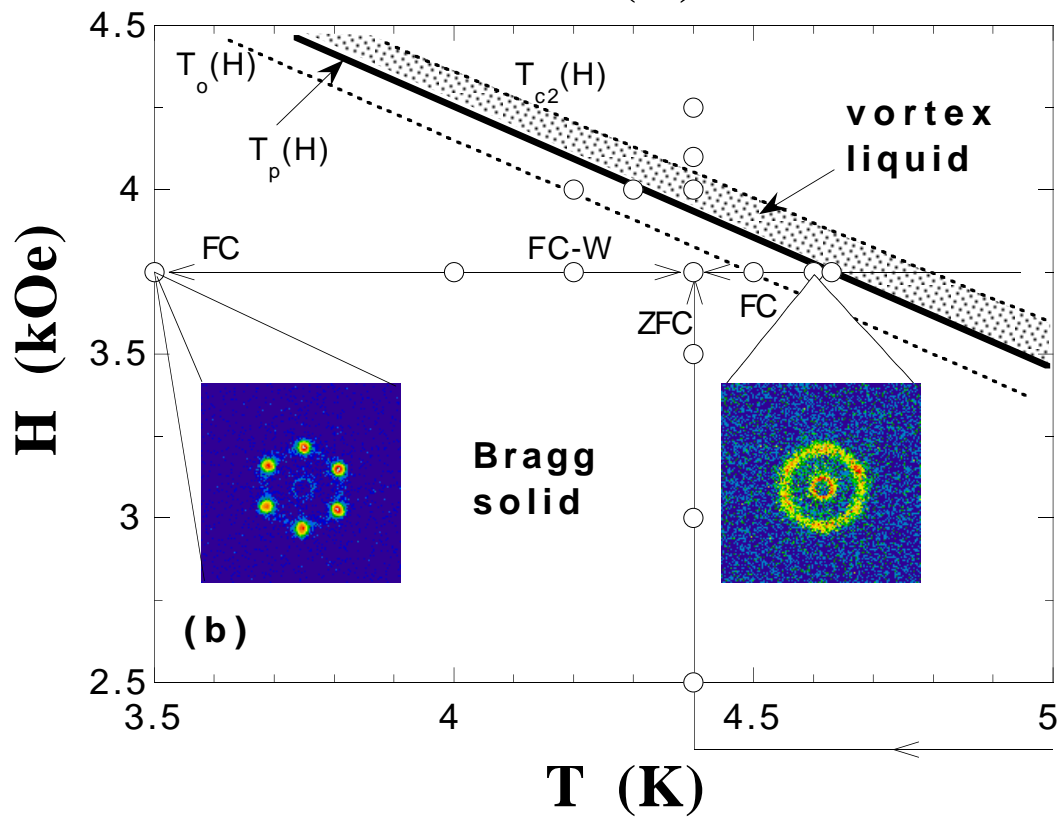
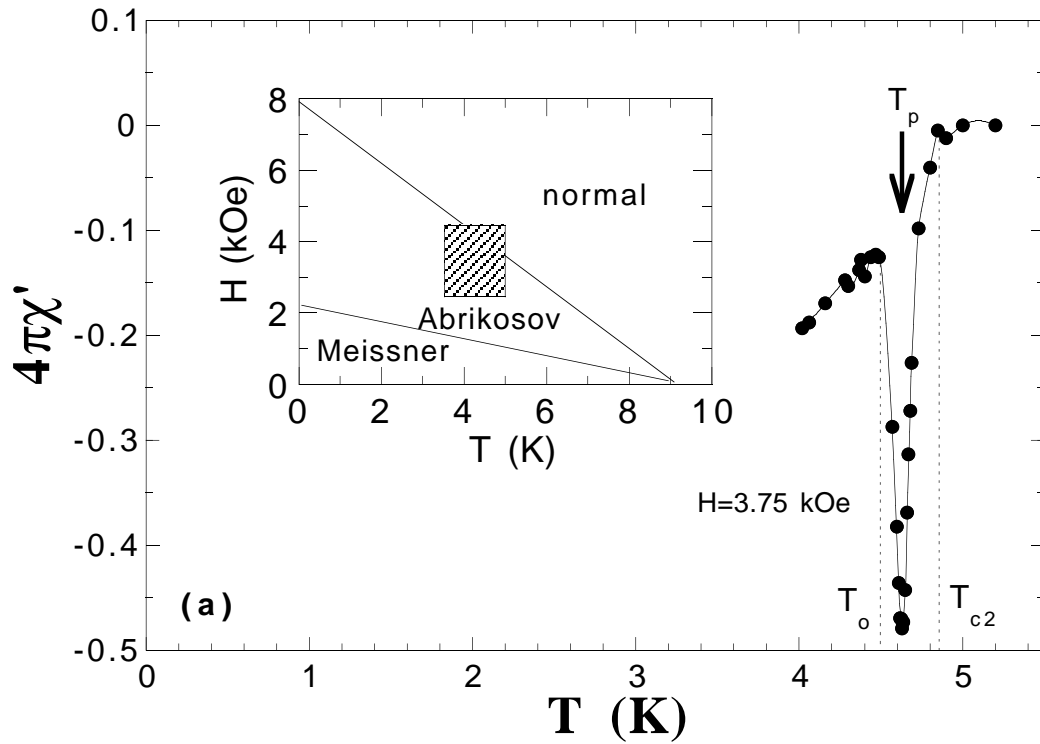
Fig.1: Peak effect and the field-temperature ($H - T$) phase diagram of Nb. (a) Representative ac magnetic susceptibility $\chi'(T)$ vs. T for $H_{dc}=3.75$ kOe (field-cooled). $H_{ac}=3.3$ Oe and $f=1.0$ kHz. $H_{dc}||H_{ac}$. (For details on ac magnetic measurements, see [5,8].) Inset: the global $H - T$ phase diagram for the Nb crystal used in this study. (b) Expanded view of the $H - T$ phase diagram for Nb (the shaded box in (a)). Two representative SANS images of the field-cooled vortex states are shown (no background subtraction).

Fig.2: History-dependent neutron diffraction patterns. $T=4.40$ K for all images. The SANS images of the ZFC and FC vortex states for $H=3.75$ kOe (top panel: below the onset of the peak effect) and $H=4.00$ kOe (mid panel: near the upper end of the peak-effect regime). The thick arrows indicate how the SANS images evolve after applying a small ac magnetic field (see text). The lower panel shows the intensity data at the radial maximum as a function of the azimuthal angle θ for the ZFC and FC SANS data (background subtracted) at $H=4.00$ kOe and $T=4.40$ K.

Fig.3: Temperature dependence of the SANS widths. (a) The azimuthal widths of the Bragg peaks at Q_o and (b) the radial widths vs. reduced temperature for ZFC, FC, and FC-W vortex states. The FC-W data points at 3.75 kOe and 4.40 K are indicated by the crosses (and marked by arrows). The instrumental resolution in width is marked in (a). The lines are guides for the eye. The dashed lines indicate $T_p(H)$.

Fig.4: The effect of an ac field, $H_{ac}=3.3$ Oe and $f=100.0$ Hz, on the ordered ZFC state for $H=4.00$ kOe and $T=4.40$ K (above $T_p(H)$). (a) $I(Q_o)$ vs. azimuthal angle; (b) the intensity $I(Q)$ (averaged over the azimuthal

angle) as a function of the momentum transfer Q . The location of the radial maximum Q_o is found by fitting $I(Q)$ to a Gaussian. The lines are Gaussian fittings.



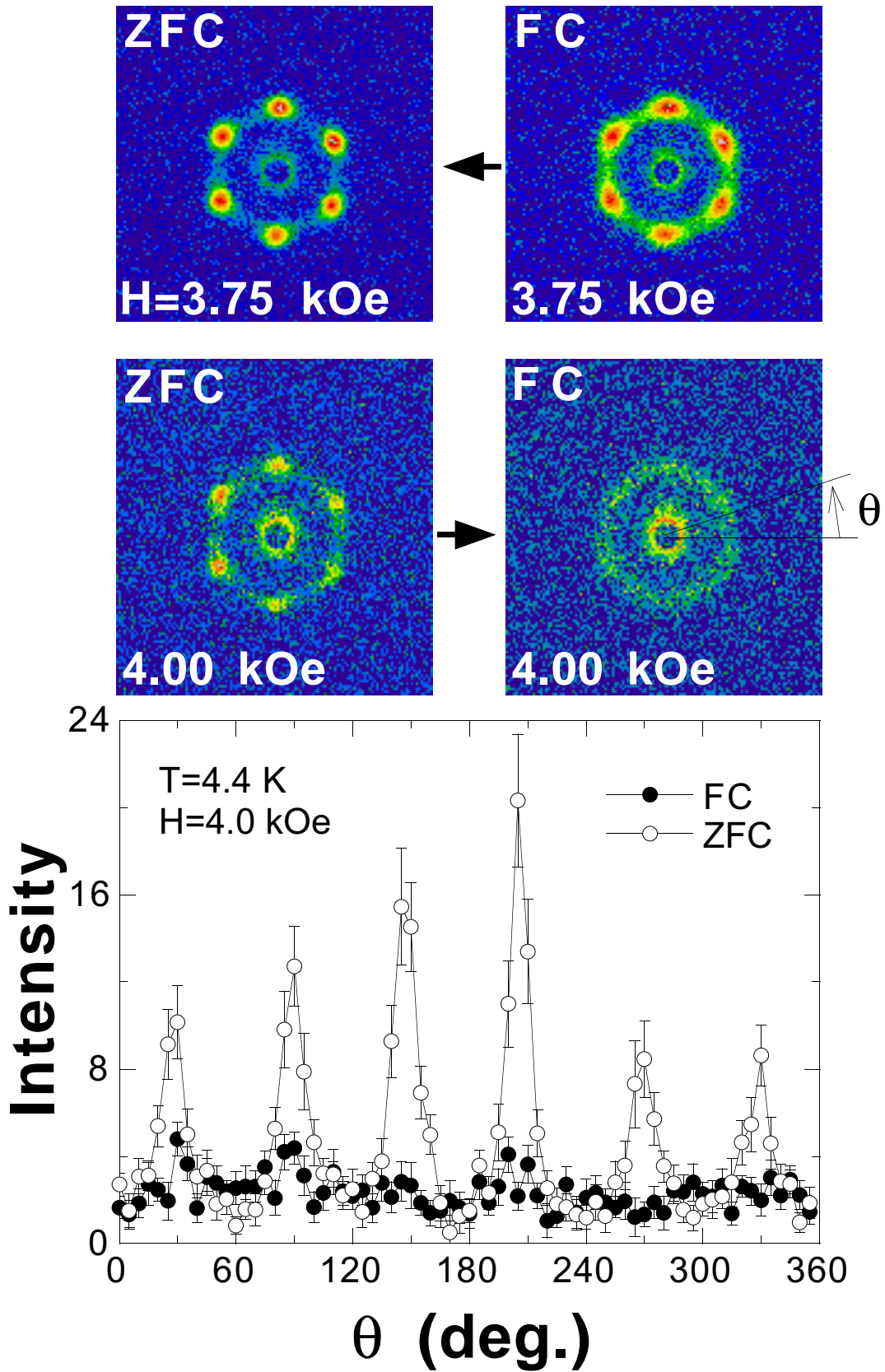


Fig.2 (color) Ling et al.

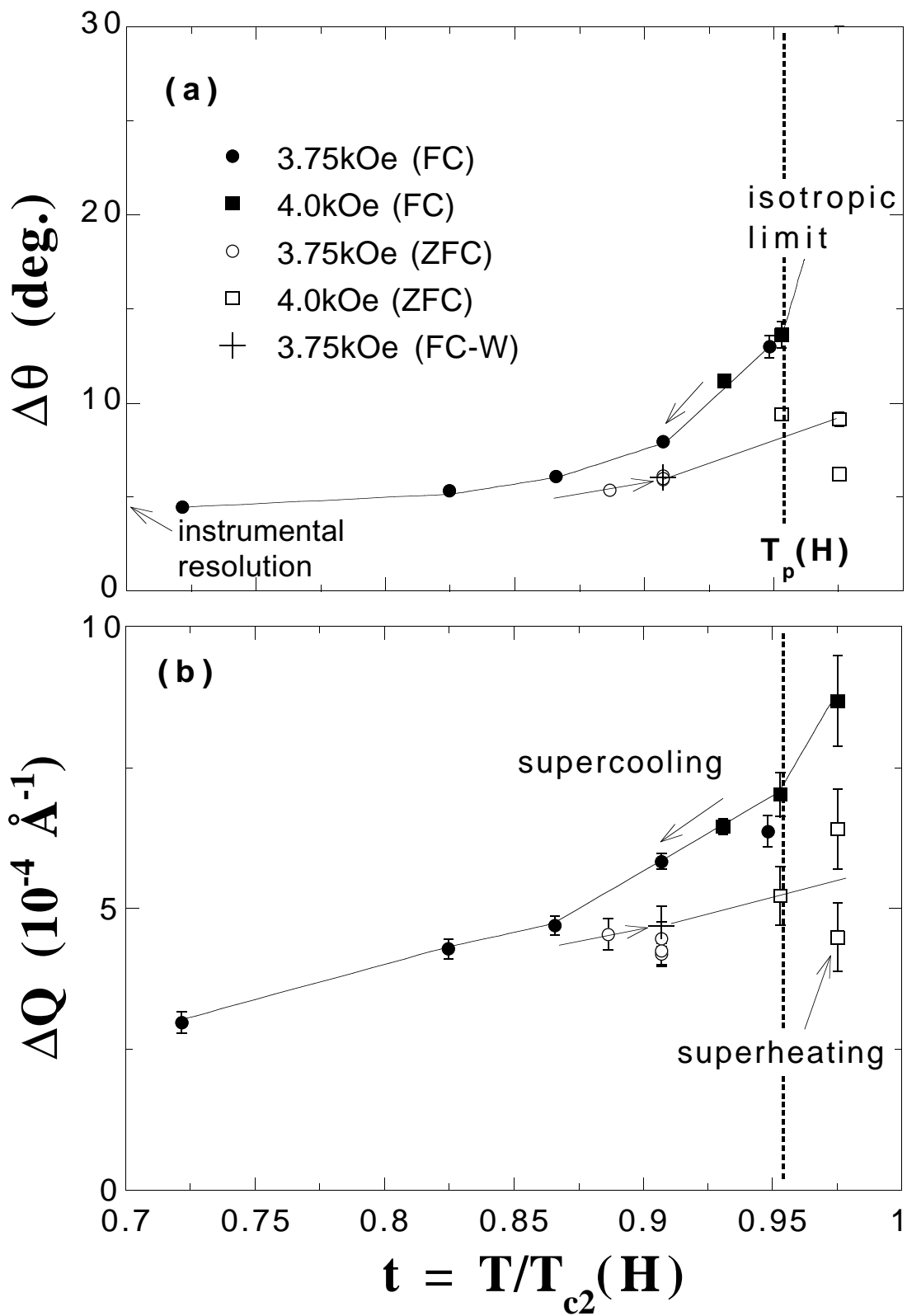


Fig.3 Ling et al.

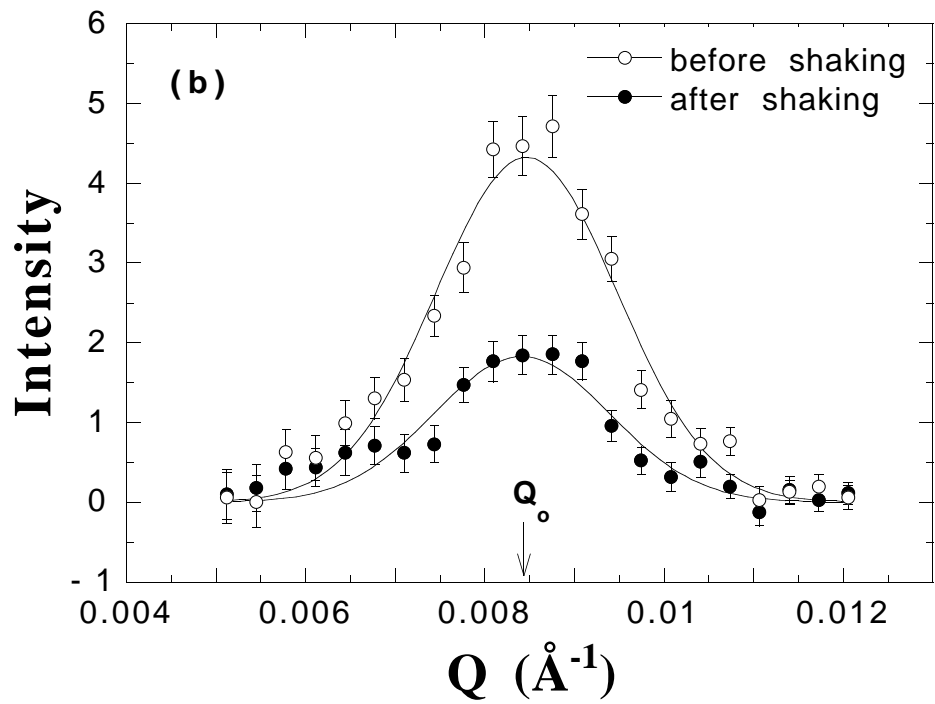
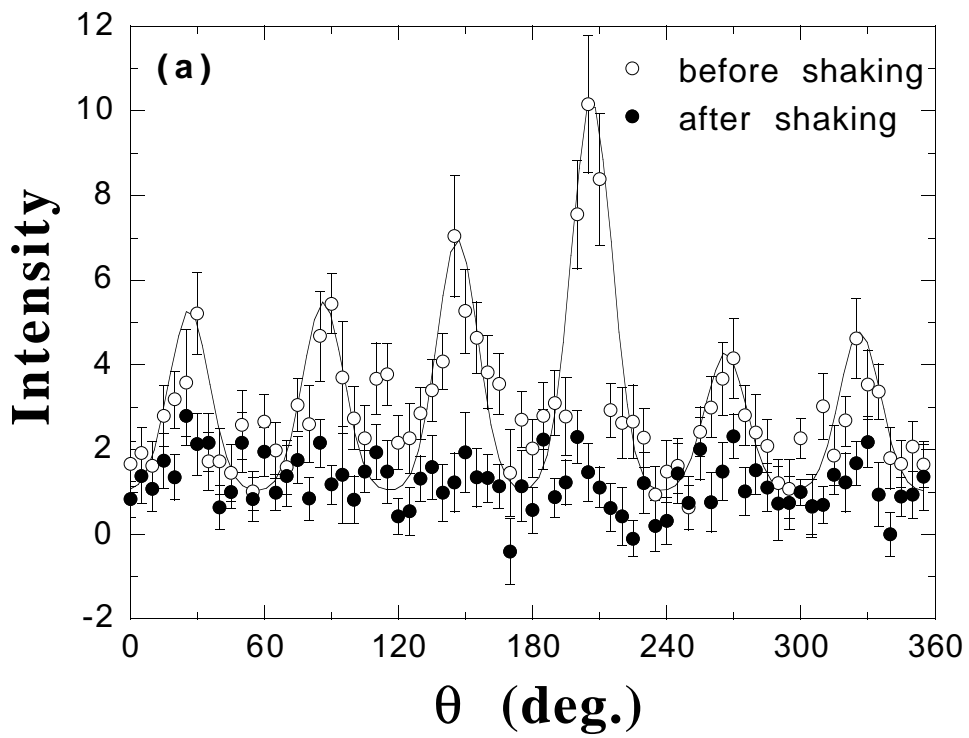


Fig.4 Ling et al.